Mean Concentrations and Concentration Fluctuations in a Stirred-Tank Reactor

Iris L. M. Verschuren, Johan G. Wijers, and Jos T. F. Keurentjes
Eindhoven University of Technology, Dept. of Chemical Engineering and Chemistry, Process Development Group, 5600 MB Eindhoven, The Netherlands

Mixing has a major influence on the product ratio of fast competitive reactions, as the product ratio of these reactions is determined by local concentrations. To integrate models from literature for the description of the mean and fluctuating concentration of a continuous reactant flow fed to a stirred-tank reactor, the models are validated against detailed experimental data for a stirred-tank reactor equipped with a Rushton turbine impeller. Application of these models requires information on local hydrodynamic parameters, which are determined by laser Doppler velocimetry. Model calculations are validated by determining the mean concentration and concentration variance of an inert tracer fed with planar laser-induced fluorescence to the studied stirred-tank reactor. To calculate the mean concentration, a combination of a theoretical model, measured mean concentrations and LDV measurements is used to determine the turbulent diffusion coefficient. The turbulent mixer model is used to calculate the concentration variance. Compared to the literature, this model requires adjustment of the constant in the production of the concentration variance to fit the measured concentration variances correctly. For the mean concentration and its variance, measurements agreed reasonably with simulations.

Introduction

Before a chemical reaction can take place, the reactants have to be mixed on a molecular scale. Inefficient mixing has major negative effects on the yield and selectivity of a broad range of chemical reactions, because slow mixing can retard desired reactions and promote undesired side reactions. A well-designed and controlled mixing process leads to significant pollution prevention, better usage of raw materials and the prevention of byproduct formation avoids expensive separation costs downstream in the process. An example of a mixing-sensitive process is the addition of an acid or base to an organic substrate, which degrades in the presence of a high or low pH. Slow mixing will limit the neutralization reaction, which will allow the organic substrate to react with the acid or base to unwanted byproducts (Paul et al., 1992). Other examples of mixing-sensitive processes are various types of polymerizations, precipitations, and fermentations (e.g., Fields and Ottino, 1987; Franke and Mersmann, 1995; Larsson et al., 1992).

Correspondence concerning this article should be addressed to I. L. M. Verschuren.

The selectivity of a mixing-sensitive reaction depends on local concentrations inside a reactor. This study is focused on determining local concentrations in stirred-tank reactors operated under turbulent flow conditions, as it is often used in the chemical and biochemical industry. In principle, local properties of a flow, such as velocity or concentration, are described by the conservation equations of mass, momentum, and energy. Since turbulent flows of practical interest contain a wide range of time and length scales, the complete exact solution of these equations is not possible with the computational resources available today. Therefore, simplified but tractable models are proposed in the literature to describe the mixing in turbulent flows. The most widely accepted approach for modeling the mixing in a turbulent flow is based on Reynolds decomposition (Fox, 1996). Reynolds decomposition consists of describing a property of the turbulent flow with a mean and a fluctuating value. These models have been verified for a tubular reactor by comparing model predictions with experimentally determined yields of a test reaction (Baldyga, 1989; Baldyga and Henczka, 1997; Hannon et al., 1998). The objective of this work is to integrate models from litera-

ture, allowing for the description of the mean and fluctuating concentration of an inert tracer fed to a stirred-tank reactor. Models that employ the concept of turbulent diffusivity will be validated against experimental data and will be refined to make them more suitable for stirred-tank reactors. The models used to describe the mean concentration and concentration variance require information about local hydrodynamic parameters. In this study, these parameters have been determined for a stirred-tank reactor equipped with a Rushton turbine impeller using laser Doppler velocimetry (LDV). To validate the simulations, mean concentrations and concentration variances of an inert tracer fed to the same stirred-tank reactor have been measured with planar laser-induced fluorescence (PLIF).

Model for Mean Concentration and Its Variance of an Inert Tracer Fed to a Stirred-Tank Reactor

Reynolds decomposition and time averaging applied to the mass-transfer equation of an inert tracer result in

$$\frac{D\bar{c}}{Dt} = \frac{\partial}{\partial x_j}\left[(D_m + D_T)\frac{\partial \bar{c}}{\partial x_j}\right], \tag{1}$$

where $\bar{c}$ is the time-averaged concentration of an inert tracer, x is a space coordinate, D_m is a molecular diffusion coefficient, and D_T is the turbulent diffusion coefficient. In this study, Eq. 1 is used to describe the mean concentration field of a continuous feed stream in a stirred-tank reactor. As noticed by Baldyga and Pohorecki (1995), in a continuous feedstream the concentration gradients in the radial direction are much larger than the concentration gradients in the direction of the flow. Therefore, only radial dispersion is assumed. Molecular diffusion has been assumed to be negligible compared to turbulent diffusion.

The turbulent diffusion coefficient depends on the velocity and the length scale of the turbulent motions taking part in the turbulent diffusion process (Tennekes and Lumley, 1972)

$$D_T \approx u(\lambda)\cdot\lambda, \tag{2}$$

in which the length scales and the velocities of the turbulent motions are assumed to be described by a characteristic length scale (λ) and a characteristic velocity [$u(\lambda)$], respectively. The characteristic velocity of a turbulent motion is described by the energy dissipation rate (ϵ) and the characteristic length scale (Tennekes and Lumley, 1972)

$$u(\lambda) \approx (\epsilon\cdot\lambda)^{1/3}. \tag{3}$$

Substituting Eq. 3 into Eq. 2 leads to the following equation for the turbulent diffusion coefficient

$$D_T = A\epsilon^{1/3}\lambda^{4/3}, \tag{4}$$

with A being a constant.

The value of λ depends on the relative size of the scalar cloud compared to scales of the turbulent flow field (Lesieur, 1990). When the concentration scales are equal to or larger than the scales of the turbulent flow field, λ is equal to the integral velocity length scale and the constant A is equal to 0.1 (Baldyga and Pohorecki, 1995). Usually, a feedstream is introduced into a stirred tank reactor with an initial concentration length scale smaller than the scales of the turbulent flow field. In that case, λ will be equal to a characteristic length scale describing the size of the scalar cloud. In this work λ is assumed to be equal to the radius of the feedstream when this radius is smaller than the integral velocity length scale. In the literature the constant $A = 0.1$ is used (Baldyga and Pohorecki, 1995). As $A = 0.1$ results from empirical constants in the k-ϵ model, in this study the value for the constant A has been determined by optimizing the agreement between measured and calculated mean concentration profiles.

The radius of the feedstream is calculated as follows. A scalar length scale (L), such as the radius of a feed stream, which is smaller than the integral velocity length scale follows the Richardson law (Lesieur, 1990)

$$\frac{1}{2}\frac{dL^2}{dt} = C\epsilon^{1/3}L^{4/3}. \tag{5}$$

The value of C depends on the length scale taken into consideration. If L corresponds to a scalar cloud diameter, C is equal to 2.14 (Lesieur, 1990). Integration of Eq. 5 leads to the following equation for the radius of the feedstream

$$r = \left(r_0^{2/3} + (2/3)C\epsilon^{1/3}t\right)^{3/2}, \tag{6}$$

with $C = 1.35$. This value for C corresponds to the growth of the diameter of the feed stream with a constant equal to 2.14.

Equation 1 describing the mean concentration field of a passive tracer is developed in an Eulerian frame, while Eq. 5 describes the radius of the feed stream as a function of Lagrangian time. However, the displacement of a small lump of fluid in the axial direction (z) due to the action of a turbulent motion is assumed to be small compared to the displacement in this direction due to convection with the mean velocity. With this assumption the radius of the feedstream at a certain distance z is equal to the radius at time t, with

$$t = \int_0^z \frac{1}{\overline{u_{\mathrm{ax}}}}dz \tag{7}$$

in which z is the axial distance below the feed pipe and $\overline{u_{\mathrm{ax}}}$ is the mean axial velocity below the feed pipe.

The initial radius of the feedstream (r_0) has been estimated as follows. When the momentum of the feedstream is negligible compared to the momentum of the flow in the reactor, the velocity of the feedstream will, soon after leaving the feed tube, be equal to the local circulation velocity ($\overline{u_c}$). This is normally the case when the feed velocity is smaller than or comparable to the local circulation velocity (Jeurissen et al., 1994). Under these circumstances the initial radius (r_0)

of the feed stream is given by (Baldyga et al., 1997)

$$r_0 = \sqrt{\frac{Q_{\text{feed}}}{\pi u_c}}\,, \tag{8}$$

with Q_{feed} the volumetric flow rate of the feed liquid.

The concentration variance of an inert tracer is described by the turbulent-mixer model proposed by Baldyga (1989). In this model the concentration variance (σ^2) is divided into three parts. Each part corresponds to one of the mixing processes in a turbulent flow for Schmidt numbers much larger than one. These mixing processes and corresponding range of length scales (l) are

(1) Inertial-convective disintegration of large eddies (σ_1^2), $L_v \le l \le 12 l_k$.

(2) Viscous-convective formation of laminated structures (σ_2^2), $12 l_k < l < l_k$.

(3) Molecular diffusion within the deforming laminates structures (σ_3^2), $l < l_k$.

The Kolmogorov length scale (l_k) is

$$l_k = \left(\frac{\upsilon^3}{\epsilon}\right)^{1/4}, \tag{9}$$

where υ is the kinematic viscosity ($\approx 10^{-6}$ for water).

The concentration variance is equal to the sum of these three parts

$$\sigma^2 = \sigma_1^2 + \sigma_2^2 + \sigma_3^2. \tag{10}$$

In this article the spatial resolution of the measurements was sufficient to measure the inertial-convective variance component. The transport equation for this component of the concentration variance is

$$\frac{D\sigma_1^2}{Dt} = \frac{\partial}{\partial x_j}\left[(D_m + D_T)\frac{\partial \sigma_1^2}{\partial x_j}\right] + R_{p1} - R_{D1}, \tag{11}$$

in which R_{p1} is the production rate and R_{D1} is the dissipation rate.

According to Spalding (1971), the production rate of the concentration variance in the inertial-convective subrange of wave numbers (σ_1^2) is

$$R_{p1} = C_{g1} D_T \left(\frac{\partial \bar{c}}{\partial x_j}\right)^2 \tag{12}$$

with C_{g1} being a constant. A commonly used value for this constant is about 2 (Fox, 1996; Baldyga and Henczka, 1997; Spalding, 1971).

The decay of σ_1^2 by the inertial-convective distintegration of large eddies is described by Corrsin (1964) and Rosenweig (1964)

$$R_{D1} = \frac{\sigma_1^2}{\tau_s} \tag{13}$$

$$\tau_s = 2\left(\frac{L_c^2}{\epsilon}\right)^{1/3} \tag{14}$$

where L_c is the scalar integral length scale. The initial scalar integral length scale is set equal to the initial radius of the feed stream (r_0) (Baldyga et al., 1997). This length scale will grow according to Eq. 5, with $C = 0.3$ (Lesieur, 1990).

The calculation of mean concentrations and concentration variances with the equations just given requires information about the local energy dissipation rate and local circulation velocity. In this study, local energy dissipation rates and circulation velocities have been determined experimentally using LDV for a stirred-tank reactor equipped with a Rushton turbine impeller. To validate the simulations, mean concentrations and concentration variances have been measured with PLIF at various axial locations below the feed pipe inside the stirred-tank reactor studied.

Local Energy Dissipation Rates and Mean Velocities

LDV experiments

LDV was used to determine local velocities and energy dissipation rates. The vessel used for these LDV experiments was made of Perspex and was equipped with a standard six-bladed Rushton turbine impeller, four baffles, a feed pipe, and an effluent pipe. The geometry of the tank is shown in Figure 1. The internal diameter of the vessel (T) was 0.288 m. The internal diameter of the feed pipe was 8 mm. The wall thickness of the feed pipe was about 1 mm. Details of the impeller geometry are given in Figure 2.

A commercially available LDV setup was used, operating in the backscatter mode with two beam pairs. The LDV setup consisted of a 2-W argon laser (Stabilite 2017 by Spectra Physics), a color separator, photomultipliers, burst spectrum

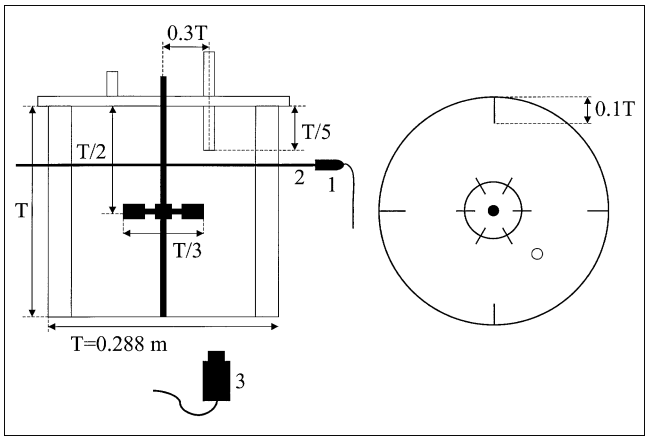

Figure 1. Stirred vessel and experimental setup used for planar laser-induced fluorescence experiments:

1. laser probe; 2. laser light sheet; 3. high-speed CCD camera.

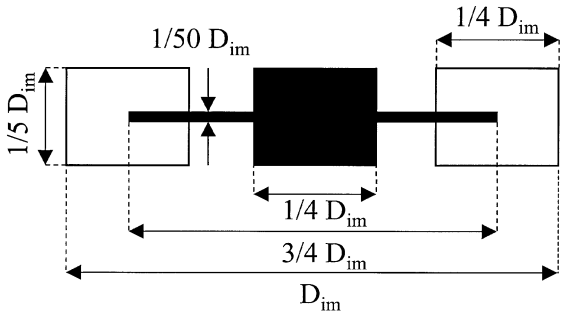

Figure 2. Rushton turbine impeller showing the dimensions.

analyzers (Dantec), and a probe attached to an automated transverse system. The wavelengths of the beam pairs were 488 nm and 514.5 nm, respectively. To be able to discriminate between the positive and negative directions of the velocity, one beam of each pair was given a frequency shift of 40 mHz. The measuring volume created by the intersection of two laser beams of the same wavelength was 3 mm in length and 0.15 mm in diameter (see Figure 3).

The stirred-tank reactor was entirely filled with water and seeded with a small amount of dispersed polystyrene latex with an average particle size of 4 μm. The reactor was placed in a rectangular glass tank filled with water to reduce the diffraction of the laser light due to the curvature of the reactor surface.

LDV measurements were performed for a stirrer speed of 3.1 Hz at four positions on a vertical line below the feed pipe, as illustrated in Figure 3. The velocities and the energy dissipation rates were normalized with the stirrer tip velocity (v_{tip}) and the average energy dissipation rate inside the stirred-tank reactor ($\bar{\epsilon}$), respectively. The average energy dissipation rate inside the stirred-tank reactor is estimated using:

$$\bar{\epsilon} = \frac{N_p N^3 D_{\text{im}}^5}{V_{\text{reactor}}}, \tag{15}$$

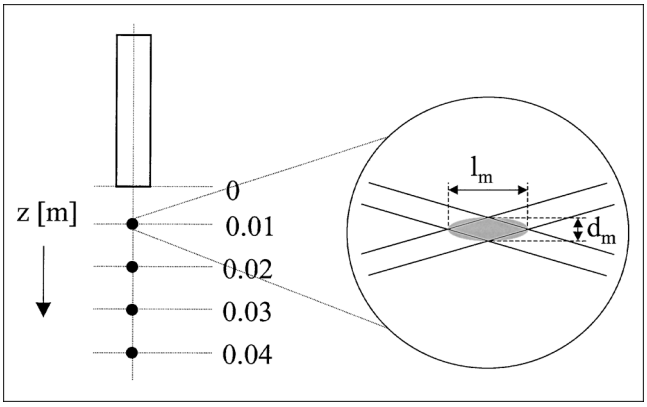

Figure 3. Measurement positions for laser Doppler velocimetry experiments, and LDV measurement volume.

in which N_p is the power number equal to 5.3 for the Rushton turbine impeller used in this work (Schoenmakers, 1998), N is impeller speed, D_{im} is impeller diameter, and V_{reactor} is the liquid volume inside the reactor.

LDV data processing

LDV is based on the measurement of the velocities of the particles suspended in the flow. The higher measurement probability of particles with a higher velocity yields a velocity distribution biased toward higher values. In order to eliminate this velocity bias, transit time weighting was applied when calculating the mean velocity ($\bar{u}_i$) and the mean square fluctuating velocity ($\overline{u_i'^2}$):

$$\bar{u}_i = \sum_{j=0}^{N-1} \eta_j u_{ij} \tag{16}$$

$$\overline{u_i'^2} = \sum_{j=0}^{N-1} \eta_j \left(u_{ij} - \bar{u}_i\right)^2 \tag{17}$$

$$\eta_j = \frac{t_j}{\sum_{k=0}^{N-1} t_k}, \tag{18}$$

where t_j is the transit time of a particle crossing the measurement volume and u_{ij} is the velocity of this particle.

The energy dissipation rate was estimated with

$$\epsilon = \beta \frac{k^{3/2}}{L_v}, \tag{19}$$

in which β is a constant, equal to unity (Kusters, 1991), k is the turbulent kinetic energy, and L_v is the integral velocity length scale.

The turbulent kinetic energy was calculated from the velocity fluctuations in the three orthogonal directions

$$k = \frac{1}{2} \sum_{i=1}^{3} \overline{u_i'^2}. \tag{20}$$

The integral length scale was calculated from the integral time scale (T_v) using Taylor's hypothesis

$$L_v = \sqrt{\sum_{i=1}^{3} \overline{u_i}^2} \cdot T_v. \tag{21}$$

The integral time scale is equal to the sum of the time scales for the three orthogonal directions (T_i)

$$T_v = \sum_{i=1}^{3} T_i. \tag{22}$$

These time scales were calculated from the energy spectrum of the velocity fluctuations [$E_i(f)$] (Hinze, 1975)

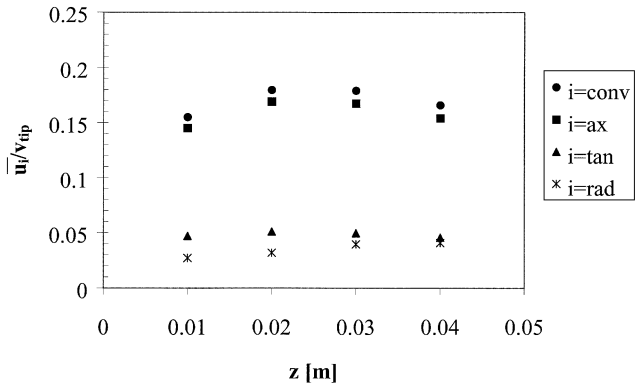

Figure 4. Mean velocities normalized to stirrer tip speed in the radial, axial and tangential direction and normalized convection velocity as a function of the axial distance below the feed pipe.

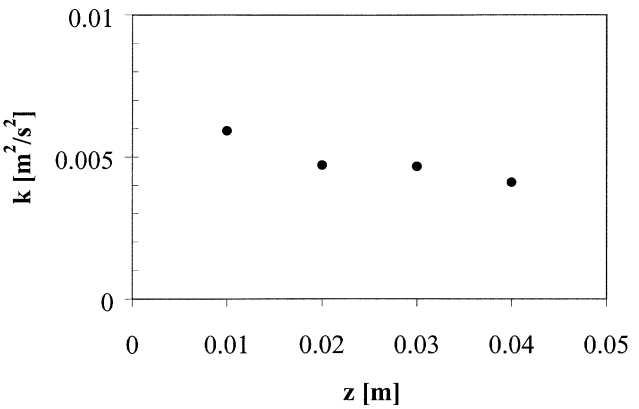

Figure 5. Turbulent kinetic energy below the feed pipe as a function of the axial coordinate, for stirrer speed of 3.1 Hz.

$$T_i = \frac{1}{\overline{u_i'^2}} \lim_{f \to 0} E_i(f). \tag{23}$$

The integral time scale was approximated from the average of the first points obtained in the horizontal part of the energy spectrum.

To calculate an energy spectrum, discrete velocity samples have to be evenly distributed in time. To obtain evenly distributed velocity samples from the LDV-measurements, the sample–hold technique was used (Adrian and Yao, 1987)

$$u_{SH}(t) = u(t_j) \qquad t_j \le t < t_{j+1}. \tag{24}$$

The energy spectrum was calculated from the autocovariance of the velocity fluctuations [$C_{u_iu_i}(\tau)$] using fast fourier transformation

$$C_{u_iu_i}(\tau) = \lim_{T \to \infty} \frac{1}{T} \int_0^T \left(u_i(t) - \overline{u_i}\right)\left(u_i(t+\tau) - \overline{u_i}\right) dt \tag{25}$$

$$E_i(f) = \int_{-\infty}^{\infty} C_{u_iu_i}(\tau) e^{-i2\pi f\tau} d\tau. \tag{26}$$

Results of the LDV experiments

Figure 4 shows the mean velocities in three orthogonal directions and the circulation velocity normalized with the tip velocity as a function of the axial coordinate. The mean velocity in the axial direction is approximately equal to the circulation velocity, whereas the mean velocities in radial and tangential direction are significantly smaller. In Figure 5, turbulent kinetic energies are given as a function of the axial distance below the feed pipe. Velocity length scales have been calculated from integral time scales, which have been approximated from the average of the first points obtained in the horizontal part of the energy spectrum. Figure 6 shows a representative example of an energy spectrum obtained from measured axial velocities at 0.03 m below the feed pipe. In Figure 7, normalized velocity length scales (L_v/T) are presented as a function of the axial distance below the feed pipe.

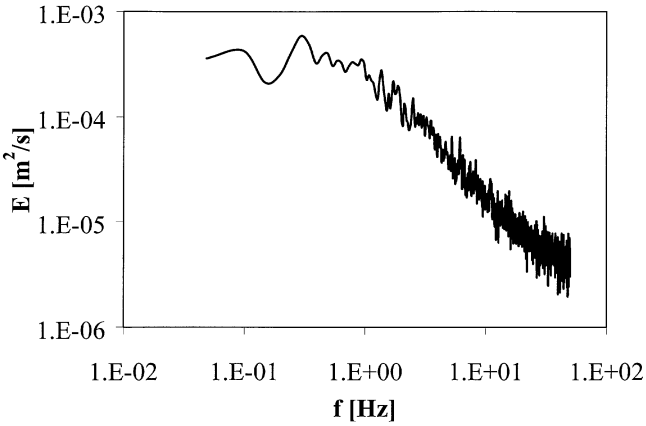

Figure 6. Energy spectrum obtained from measured axial velocities at 0.03 m below the feed pipe.

To simplify the calculations, average hydrodynamic parameters below the feed pipe have been used in the models to calculate local mean concentrations and concentration vari-

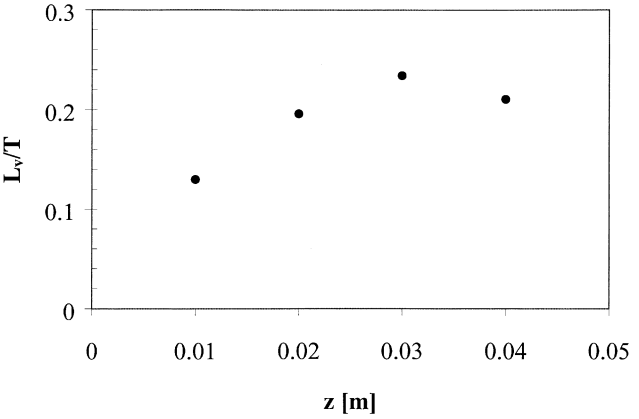

Figure 7. Velocity length scales normalized to the vessel diameter as a function of the axial distance below the feed pipe.

Table 1. Hydrodynamic Parameters Averaged Over the Axial Distance Below the Feed Pipe

Hydrodynamic Parameters	Avg. Value
$\overline{u_{ax}}$	0.16 v_{tip}
$\overline{u_c}$	0.17 v_{tip}
k	0.005 m^2/s^2
L_v	0.19 D
ϵ	0.1 $\bar{\epsilon}$

ances. These average hydrodynamic parameters have been obtained by averaging the hydrodynamic parameters measured over the axial distance with LDV, and are presented in Figures 4, 5, and 7. The averaged hydrodynamic parameters are given in Table 1. The average energy dissipation rate below the feed pipe has been calculated by substituting the average kinetic energy and the average length scale in Eq. 19. This average energy dissipation rate normalized to the average energy dissipation rate inside the stirred-tank reactor is also given in Table 1.

Mean Concentration and Its Variance of Inert Tracer Fed to Stirred Tank Reactor

PLIF experiments

Local mean concentrations and concentration variances were measured using PLIF. The PLIF experiments were performed in the same vessels as were used for the LDV experiments.

The principle of PLIF is the measurement of the fluorescence intensity of a tracer dye excited by a laser sheet. As shown in Figure 1, a CCD camera placed perpendicular to the laser sheet, is used to record the fluorescence intensity and to convert the intensity into a gray value. At low tracer concentrations, the intensity of fluorescence is linearly dependent on the concentration of the dye. When this is the case, the following equation can be used to calculate the instantaneous tracer concentration at position x, y $[c(x,y,t)]$ from the gray values (Houcine et al., 1996)

$$c(x, y, t) = \frac{G(x, y, t) - \overline{G_B}(x, y)}{\overline{G_{c_{\text{hom}}}}(x, y) - \overline{G_B}(x, y)} c_{\text{hom}}, \qquad (27)$$

where $G(x, y, t)$ is the local instantaneous gray value, $\overline{G_B}(x, y)$ is the local average gray value of the background, and $\overline{G_{c_{hom}}}(x, y)$ is the local average gray value corresponding to a known tracer concentration (c_{hom}) in a homogeneous solution.

The fluorescent dye used in this study was Fluorescein. Preliminary experiments were carried out in the reactor in order to determine the range of linear response between gray value and Fluorescein concentration. In each of these experiments the reactor was filled with a Fluorescein solution of known concentration, and gray values were determined at several positions in the tank. These experiments showed that for concentrations of Fluorescein of less than 6×10^{-8} mol/L, the gray value was linearly related to the Fluorescein concentration.

A laser beam with a wavelength of 488 nm was formed into a sheet of 0.5 mm thickness using a cylindrical lens (Dantec 9080XO.21). The laser sheet was placed horizontally in the vessel, as shown in Figure 1. Before each experiment, the reactor was entirely filled with water. During an experiment, a Fluorescein solution was injected into the reactor with a velocity approximately equal to the local circulation velocity

$$v_{\text{feed}} = 0.15\pi N D_{\text{im}} \qquad (28)$$

Measurements were taken at four horizontal cross sections located at 0.005 m, 0.015 m, 0.03 m, and 0.04 m below the feed pipe. The impeller speeds used were 1.5, 3 and 4 Hz. Accordingly, the feed flow rates were 3.4×10^{-6} $m^3\cdot s^{-1}$, 6.8×10^{-6} $m^3\cdot s^{-1}$, and 9.0×10^{-6} $m^3\cdot s^{-1}$, respectively. A CCD-camera (JAI CV-M30) placed perpendicularly to the plane of the laser sheet was used to record 2000 images of the feedstream during 20 circulation times. The following equation was used to calculate the circulation time

$$t_c = \frac{V_{\text{reactor}}}{r_c N_q N D_{\text{im}}^3}, \qquad (29)$$

where N_q is the pump number and r_c is the circulation ratio. The pump number and the circulation ratio were 0.7 and 3, respectively, for the Rushton turbine impeller used in this work (Schoenmakers, 1998).

The average background gray value ($\overline{G_B}$) and the average gray value of a homogeneous Fluorescein solution ($\overline{G_{c_{hom}}}$) were determined for each experiment. The average background gray value was obtained from 100 recorded images of the reactor filled with water. The average gray value of a homogeneous Fluorescein solution was obtained from 100 recorded images of the reactor filled with a Fluorescein solution of known concentration.

PLIF data processing

Feed streams inside stirred-tank reactors have been shown to oscillate (Schoenmakers et al., 1997; Houcine et al., 1999). Large-scale oscillations were also observed visually during the PLIF experiments described in this article. These oscillations are ignored in the models presented in the literature, because usually the mixing of one feed stream with a relatively homogeneous bulk liquid is investigated. Under these circumstances, the oscillations of a feedstream will have no effect on the mixing rate. To be able to compare the measured mean concentrations and concentration variances with the theoretical predictions, the influence of the oscillations on the measured mean concentrations and concentration variances was removed by assuming that the center of mass of an instantaneous radial cross section of the feed stream was located at a fixed position in the plane of measurement (Lozano et al., 1986). These centers of mass were determined automatically using the commercially available image analysis program Optimas.

Equation 27 was used to calculate the instantaneous Fluorescein concentration at each (i,j) pixel. The mean concentration and concentration variance at each (i,j) pixel were

Table 2. Spatial Resolution of PLIF Images

N (Hz)	Δx (10^{-4} m)	Δy (10^{-4} m)	l_k (10^{-4} m)	$12lk$ (10^{-3} m)	N_x	N_y	Δx_{cor} (10^{-3} m)	Δy_{cor} (10^{-3} m)
1.5	3	6	1.9	2.3	8	4	2.4	2.4
3	3	6	1.1	1.3	4	2	1.2	1.2
4	3	6	0.9	1.1	4	2	1.2	1.2

calculated with:

$$\bar{c}(i,j) = \frac{1}{N_e}\sum_{n=1}^{N_e} c(i,j) \tag{30}$$

$$\sigma^2(i,j) = \frac{\sum_{n=1}^{N_e}\left[\bar{c}(i,j) - c(i,j)\right]^2}{N_e}, \tag{31}$$

in which N_e is the total number of images per experiment.

The concentration variance components and corresponding ranges of length scales were described in the section titled "Model for the Mean Concentration and Its Concentration Variance of an Inert Tracer Fed to a Stirred-Tank Reactor." In Table 2, values for the Kolmogorov length scale (l_k) and $12l_k$ are given together with the spatial resolution of the PLIF experiments. From Table 2 and the ranges of length scales given in the section just referred to, it is concluded that the spatial resolution of the PLIF measurements was sufficient to measure the inertial-convective concentration variance component and a part of the viscous-convective concentration variance component. To determine the inertial-convective component of the concentration variance from the PLIF measurements, the spatial resolution of a PLIF image must be equal to $12l_k$. PLIF images with a spatial resolution equal to $12l_k$ were obtained by averaging the gray values of a number of adjacent pixels. These numbers of adjacent pixels in the $x(N_x)$ and $y(N_y)$ direction together with the spatial resolution are also given in Table 2.

Independent of background emission, the root-mean-square gray value of the background is 8. This corresponds to a background root-mean-square variance of about 6% of the maximum corrected gray value, which is the gray value of the initial Fluorescein concentration of the feed liquid minus the gray value of the background ($\overline{G_{c_0}} - \overline{G_B}$). Thus the root-mean-square background variance (σ_B^2/c_0^2) for the normalized inertial-convective component of the concentration variance (σ_1^2/c_0^2) is of the order of 0.06 divided by the square root of N_x times N_y. Measured concentration variances were corrected for the background variance:

$$\frac{\sigma_{1c}}{c_0} = \sqrt{\frac{\sigma_1^2}{c_0^2} - \frac{\sigma_B^2}{c_0^2}}\ . \tag{32}$$

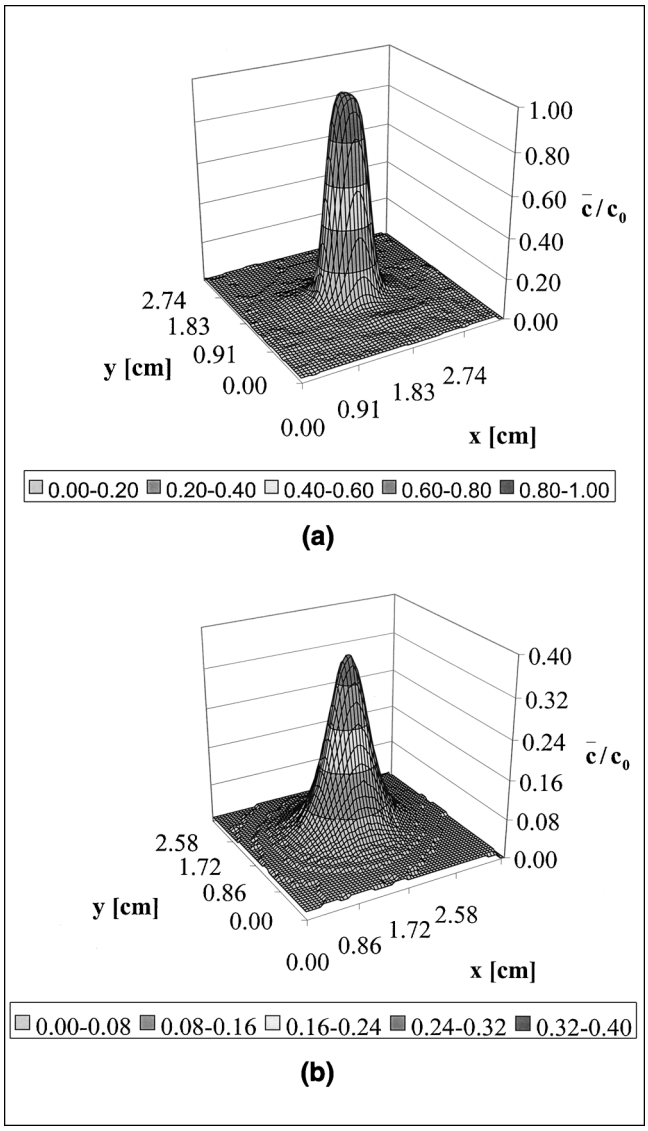

Figure 8. Measured mean concentrations at two horizontal cross sections located at (a) 0.005 and (b) 0.03 m below the feed pipe for a stirrer speed of 3 Hz.

Results of the PLIF experiments and comparison between simulations and experiments

Measured mean concentrations at two horizontal cross sections located at 0.005 m and 0.03 m below the feed pipe for a stirrer speed of 3 Hz are given in Figure 8a and 8b. Figure 9a and 9b show measured inertial-convective concentration variances at these two horizontal cross sections for a stirrer of 3 Hz. The mean concentration profiles shown in Figures 8a and 8b are both bell-shaped. Due to mixing with the environment, the height of the concentration profiles decreases and the area occupied by the feed stream increases with increasing distance from the feed pipe. At a distance of 0.005 m below the feed pipe, relatively high concentration variances are present in the periphery of the feed stream, and at the

center the concentration variances are relatively low. At a distance of 0.03 m below the feed pipe the concentration variance profile is bell-shaped, similar to the mean concentration profile. In the following, two-dimensional (2-D) cross sections of these graphs will be used for reasons of clarity.

In Figure 10a–10d, measured normalized mean concentrations ($\bar{c}/c_0$) are given for three stirrer speeds at axial distances of 0.005, 0.015, 0.03, and 0.04 m below the feed pipe. When comparing the mean concentrations measured at a certain axial distance below the feed pipe at stirrer speeds of 3 and 4 Hz, no significant variation of mean concentration with impeller speed is observed. This is in agreement with predicted mean concentrations, because the turbulent diffusion coefficient scales with impeller speed (N) and the time needed by a fluid element to flow from the feed pipe to a certain axial distance below the feed pipe is proportional to N^{-1}. However, for a stirrer speed of 1.5 Hz, the mean concentrations presented in Figure 10c and 10d are significantly higher than the mean concentrations for the other two stirrer speeds. This discrepancy may be caused by the lack of fully developed turbulence at this lower stirrer speed, whereas the model is based on fully turbulent flow conditions. Therefore, in the following, simulated mean concentrations and concentration variances will only be compared with experimentally determined values at impeller speeds of 3 and 4 Hz.

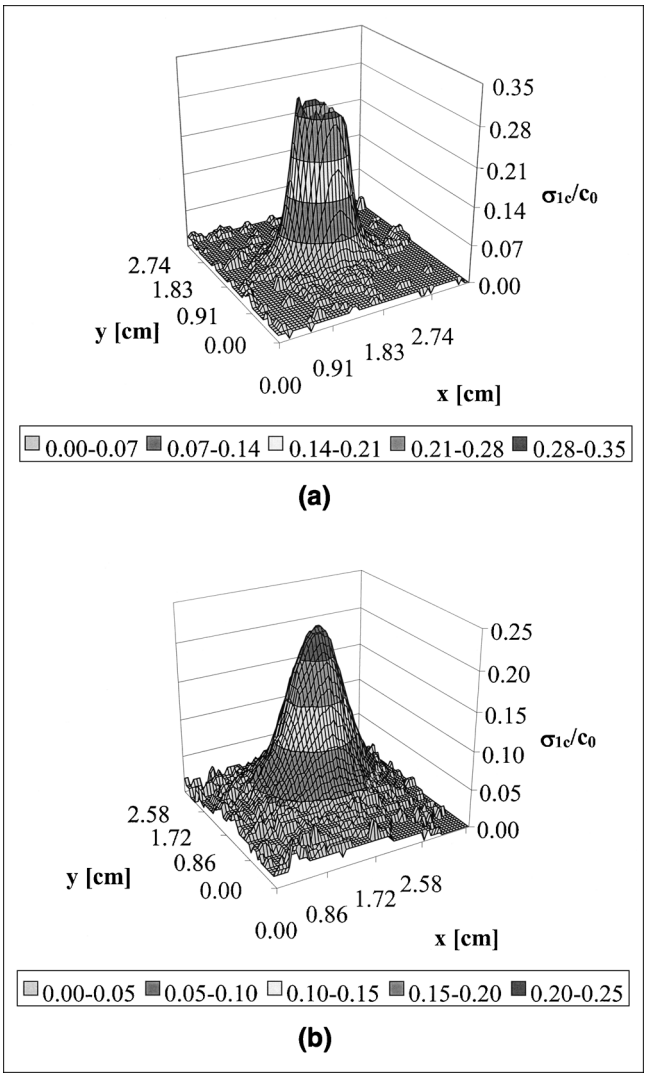

Figure 9. Measured inertial-convective concentration variances at two horizontal cross sections located at (a) 0.005 and (b) 0.03 m below the feed pipe for a stirrer speed of 3 Hz.

For the experimental conditions used in this study, the radius of the feed stream is smaller than the integral velocity length scale. In that case, the length scale (λ), used in Eq. 4 to describe the turbulent diffusion coefficient, is equal to the characteristic concentration length scale of the feed stream. In this study, λ is assumed to be equal to the local radius of the feed stream. The value for the constant A in Eq. 4 was determined by optimizing the agreement between the measured and simulated mean concentrations. Figures 10a–10d show the comparison between measured and predicted mean concentrations for impeller speeds of 3 and 4 Hz at four axial locations below the feed pipe. With the constant A equal to 0.1, the predicted mean concentrations correspond reasonably well with the measured mean concentrations. Note that this value for A is identical to values for A given in the literature for concentration length scales equal to or larger than the scales of the turbulent flow field (Baldyga and Pohorecki, 1995).

The spatial resolution of the PLIF experiments is sufficient to measure the inertial-convective part of the concentration variance. In Figure 11a–11d the root square of the measured normalized inertial-convective concentration variances corrected for the background variance (σ_{1c}/c_o) are given for three stirrer speeds at 0.005, 0.015, 0.03, and 0.04 m below the feed pipe. At a certain axial distance below the feed pipe, no significant differences between the measured concentration variances for stirrer speeds of 3 and 4 Hz are observed. This is in agreement with the model, because the turbulent diffusion coefficient scales with impeller speed (N) and the eddy disintegration time scale (τ_s) and the time needed by a fluid element to flow from the feed pipe to a certain axial distance below the feed pipe is proportional to N^{-1}.

Figure 11a–11d show the comparison between measured and predicted inertial convective concentration variances for impeller speeds of 3 and 4 Hz at four axial distances below the feed pipe. To calculate these concentration variances, the values 2 and 0.7 have been used for the constant in the production of the concentration variance (C_{g1}). As shown in Figure 11a–11d, large deviations between calculated and measured concentration variances are obtained when the value for C_{g1} that is proposed in the literature (that is, equal to 2) is used. Therefore, a value for C_{g1} equal to 0.7 has been determined by optimizing the agreement between the measured and calculated concentration variance profiles. The calculated concentration variances with $C_{g1} = 0.7$ appear to be in reasonable agreement with the experimental values. This smaller value for C_{g1} found in this work compared to the literature may result from the correction made for the large-scale oscillations of the feed stream. When no corrections for these oscillations are made, the mean concentration will be smaller and the turbulent diffusion term will be larger. The constant C_{g1} may compensate for these differences.

Conclusions and Application of Main Results

The planar laser-induced fluorescence (PLIF) technique has been successfully used to measure the mean concentration and inertial-convective concentration variance component of an inert tracer fed to a stirred-tank reactor.

For the experimental conditions used, the concentration length scales are smaller than the length scales of the turbulent flow field. Under these circumstances, the characteristic length scale and the corresponding constant to be used in the turbulent diffusion coefficient are not known from the literature. In this study, the characteristic length scale is estimated with the radius of the feed stream. A value of 0.1 for the constant in the turbulent diffusion coefficient has been obtained by optimizing the agreement between measured and predicted mean concentrations. When using this length scale and constant A, reasonably good correspondence between the measured and calculated mean concentrations is obtained.

The turbulent mixer model, used to calculate the concentration variance, requires adjustment of the constant in the production of concentration variance (C_{g1}) to obtain a reasonable agreement between the measured and predicted concentration variances. With $C_{g1} = 0.7$, the turbulent-mixer model reasonably predicts the main features of the inertial-convective component of the concentration variance.

The presumed probability-density-function (PDF) method proposed by Baldyga (1994) enables the calculation of the yield of isothermal single reactions and pairs of reactions from mean concentrations and concentration variances of an inert tracer. This method has been extended to apply to reaction schemes with an arbitrary number of steps, any number of reactants, and any reaction order or speed by the Performance Fluid Dynamics Company (Dublin, Ireland). This PDF method, combined with models from the literature describing the mean concentration and concentration variance of an inert tracer including the model refinements proposed in this study, can be used to calculate the selectivity of mixing sensitive reactions in stirred-tank reactors.

To calculate mean concentrations and concentration variances of an inert tracer with the models used in this study, we must have information about local energy dissipation rates,

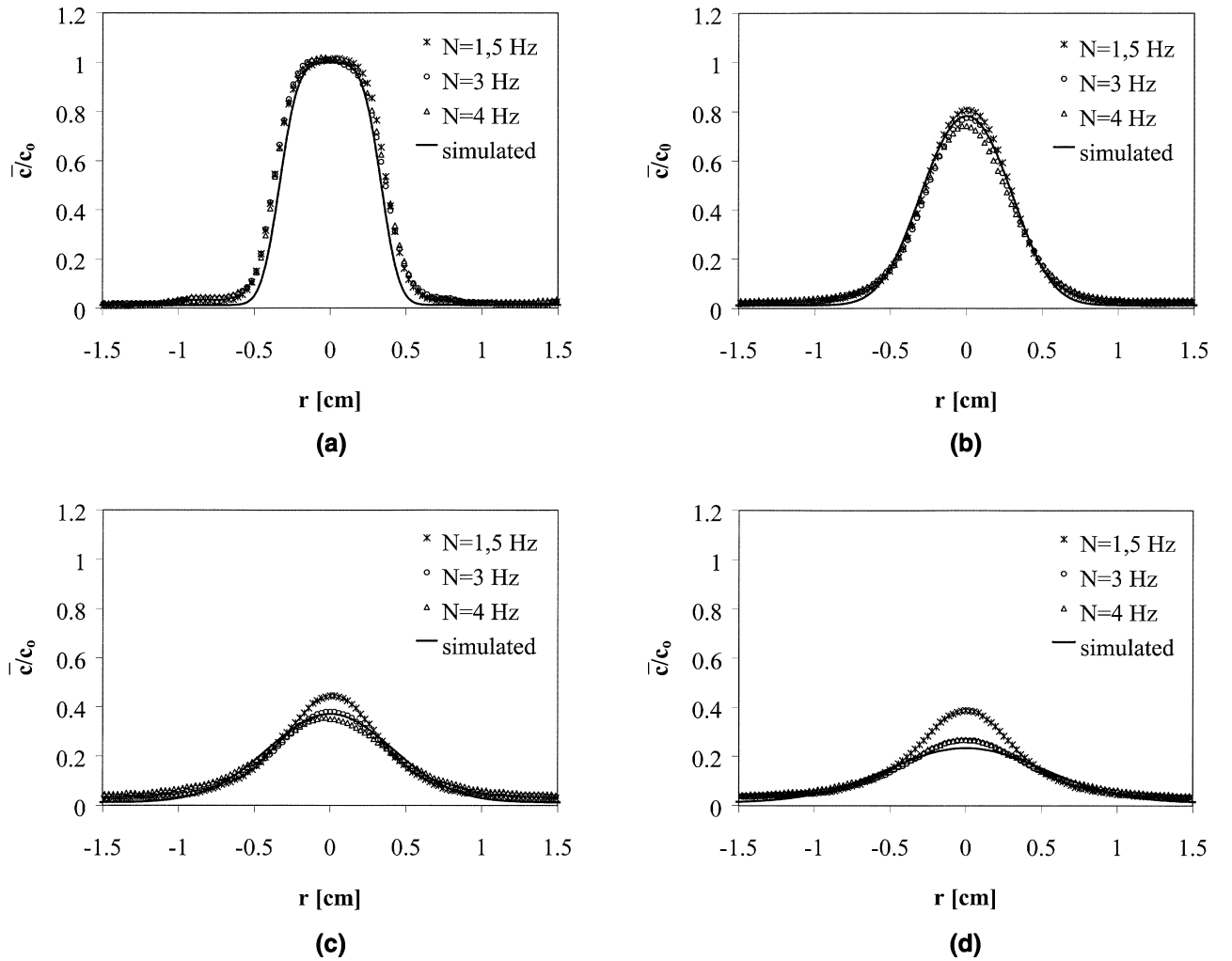

Figure 10. Measured mean concentration for a stirrer speed of 1.5, 3 and 4 Hz and predicted mean concentration profiles for a stirrer speed of 3 and 4 Hz at different axial distances below the feed pipe (z): (a) $z = 0.005$ m; (b) $z = 0.015$ m; (c) $z = 0.03$ m; and (d) $z = 0.04$ m.

velocity length scales, and velocities. A combination between information about these hydrodynamic parameters and the models for the mean concentration and concentration variance can be used to study the effect of several process and design variables on the mixing rate.

Notation

A = constant in the turbulent diffusion coefficient
c = instantaneous concentration, mol·m^{-3}
$\bar{c}$ = mean concentration, mol·m^{-3}
c' = fluctuating concentration, mol·m^{-3}
C = constant in the equation for the scalar length scale
C_{g1} = constant in the production of concentration variance
$C_{u_i u_i}$ = autocovariance of the velocity fluctuations, m^2·s^{-2}
D_{im} = impeller diameter, m
D_m = molecular diffusion coefficient, m^2·s^{-1}
D_T = turbulent diffusion coefficient, m^2·s^{-1}
E = engulfment rate, s^{-1}
$E_i(f)$ = energy spectrum, m^2·s^{-1}
f = frequency, Hz
G = instantaneous gray value
$\bar{G}$ = average gray value
G_m = molecular diffusion rate, s^{-1}
k = turbulent kinetic energy, m^2·s^{-2}
k_R = second-order reaction rate constant, m^3·mol^{-1}·s^{-1}
l_k = Kolmogorov length scale, m
L = scalar length scale, m
L_c = integral concentration length scale, m
L_v = integral velocity length scale, m
N = impeller speed, Hz
N_e = number of images
N_p = power number
N_q = pumping capacity
Q_{feed} = volumetric feed flow rate, m^3·s^{-1}
r = radius of a feed stream, m
r_c = circulation ratio
R_p = production rate of concentration variance, mol^2·m^{-6}·s^{-1}
R_D = dissipation rate of concentration variance, mol^2·m^{-6}·s^{-1}
r_0 = initial radius of a feed stream, m
Sc = Schmidt number (ν/D_m)
t = time, s
t_c = circulation time, s
T = vessel diameter, m
T_i = integral time scale for direction i, s
T_L = Lagrangian time scale, s
T_v = integral velocity time scale, s

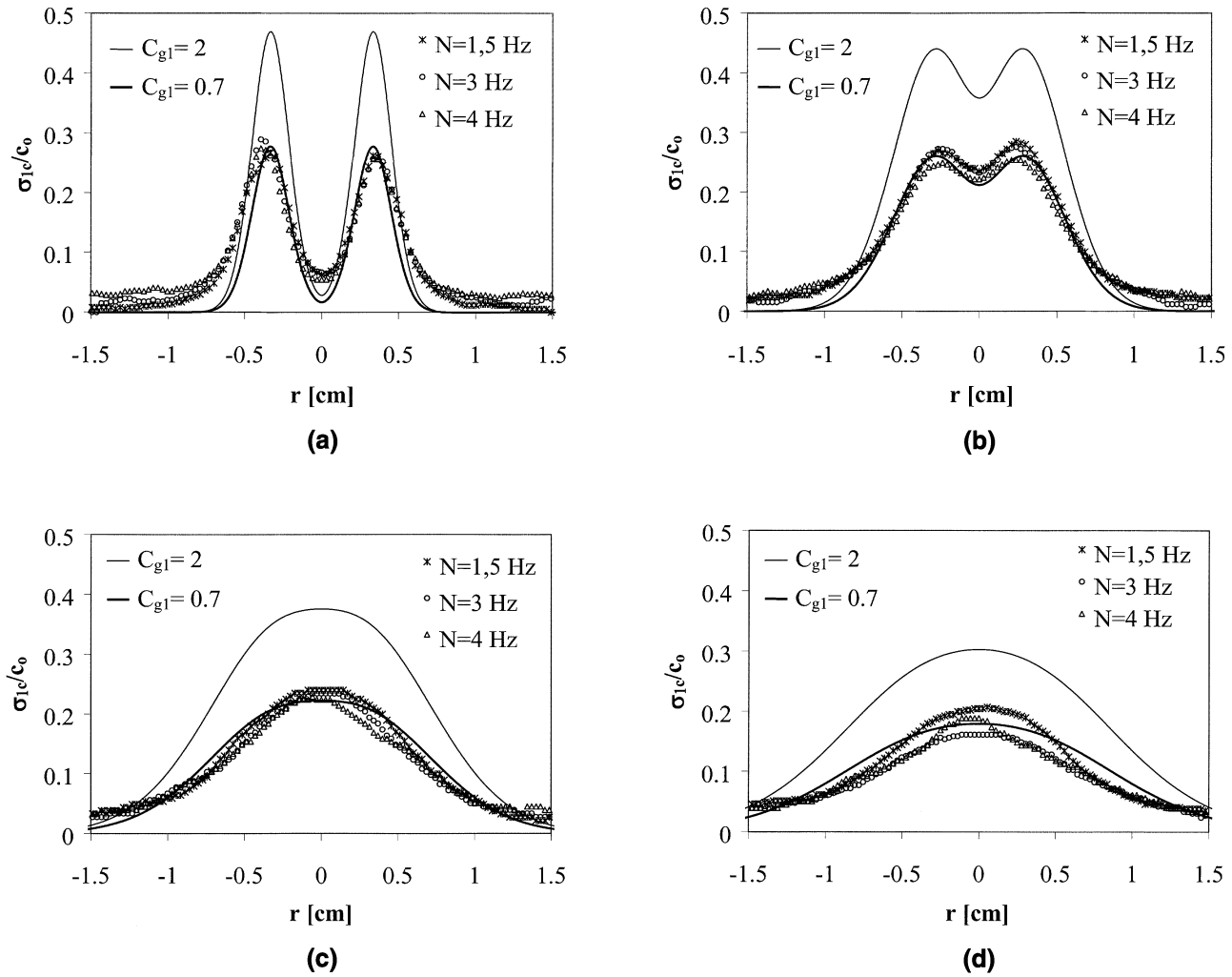

Figure 11. Inertial-convective concentration variances: measured for stirrer speed of 1.5, 3 and 4 Hz; predicted for stirrer speed of 3 and 4 Hz at different axial distances below the feed pipe (z): (a) $z = 0.005$ m; (b) $z = 0.015$ m; (c) $z = 0.03$ m; and (d) $z = 0.04$ m.

u = instantaneous velocity, $m \cdot s^{-1}$
$\bar{u}$ = mean velocity, $m \cdot s^{-1}$
u' = fluctuating velocity, $m \cdot s^{-1}$
$\overline{u_i'^2}$ = mean square fluctuating velocity, $m^2 \cdot s^{-2}$
$u(\lambda)$ = characteristic velocity of a turbulent motion, $m \cdot s^{-1}$
$\overline{u_c}$ = local circulation velocity, $m \cdot s^{-1}$
v_{feed} = feed velocity, $m \cdot s^{-1}$
V_{reactor} = reactor volume, m^3
x = space coordinate, m
z = axial coordinate, m

Greek letters

ϵ = energy dissipation rate, $m^2 \cdot s^{-3}$
η = transit-time weighting factor
$\bar{\epsilon}$ = average energy dissipation rate, $m^2 \cdot s^{-3}$
λ = characteristic length scale for turbulent diffusion, m
σ^2 = concentration variance, $mol^2 \cdot m^{-6}$
τ_s = eddy disintegration time scale, s
ν = kinematic viscosity, $m^2 \cdot s^{-1}$

Subscripts

B = background value
c_{hom} = value for a homogeneous tracer solution
i = direction
ax = axial
rad = radial
SH = sample hold
tan = tangential
0 = initial value
1 = value of variable in the inertial-convective subrange of wave numbers
2 = value of variable in the viscous-convective subrange of wave numbers
3 = value of variable in the viscous-diffusion subrange of wave numbers

Literature Cited

Adrian, R. J., and C. S. Yao, "Power Spectra of Fluid Velocities Measured by Laser Doppler Velocimetry," *Exp. Fluids*, **5**, 17 (1987).

Baldyga, J., "A Closure Model for Homogeneous Chemical Reactions," *Chem. Eng. Sci.*, **49**, 1985 (1994).

Baldyga, J., "Turbulent Mixer Model with Application to Homogeneous, Instantaneous, Chemical Reactions," *Chem. Eng. Sci.*, **44**, 1175 (1989).

Baldyga, J., J. R. Bourne, and S. J. Hearn, "Interaction Between Chemical Reactions and Mixing on Various Scales," *Chem. Eng. Sci.*, **52**, 457 (1997).

Baldyga, J., and M. Henczka, "Turbulent Mixing and Parallel Chemical Reactions in a Pipe Application of a Closure Model," *Proc. Eur. Conf. on Mixing*, **11**, 341, Paris (1997).

Baldyga, J., and R. Pohorecki, "Turbulent Micromixing in Chemical Reactors. A Review," *Chem. Eng. J.*, **58**, 183 (1995).

Corrsin, S., "Isotropic Turbulent Mixer," *AIChE J.*, **10**, 870 (1964).

Fields, S. D., and J. M. Ottino, "Effect of Segregation on the Course of Unpremixed Polymerization," *AIChE J.*, **33**, 959 (1987).

Fox., R. O., "Computational Methods for Turbulent Reacting Flows in the Chemical Process Industry," *Rev. Inst. Fr. Pet.*, **51**, 215 (1996).

Franke, J., and A. Mersmann, "The Influence of the Operation Conditions on the Precipitation Process," *Chem. Eng. Sci.*, **50**, 1737 (1995).

Hannon, J., S. Hearn, L. Marshall, and W. Zhou, "Assessment of CFD Approaches to Predicting Fast Chemical Reactions," AIChE Meeting, Miami (1998).

Hinze, J., *Turbulence*, McGraw-Hill, New York (1975).

Houcine, I., E. Plasari, R. David, and J. Villermaux, "Feedstream Jet Intermittency Phenomenon in a Continuous Stirred Tank Reactor," *Chem. Eng. J.*, **72**, 19 (1999).

Houcine, I., H. Vivier, E. Plasari, R. David, and J. Villermaux, "Planar Laser Induced Fluorescence Technique for Measurement of Concentration Fields in Continuous Stirred Tank Reactors," *Exp. Fluids*, **22**, 95 (1996).

Jeurissen, F., J. G. Wijers, and D. Thoenes, "Initial Mixing of Feed Streams in Agitated Vessels," *Inst. Chem. Eng. Symp. Ser.*, **136**, 235 (1994).

Kusters, K. A., *The Influence of Turbulence on the Aggregation of Small Particles in Agitated Vessels*, PhD Thesis, Eindhoven Univ. of Technology, Eindhoven, The Netherlands (1991).

Larsson, G., S. George, and S. O. Enfors, "Scale-Down Reactor Model to Simulate Insufficient Mixing Conditions During Fed Batch Operation Using a Biological Test System," *AIChE Symp. Ser.*, **293**, 151 (1992).

Lesieur, M., *Turbulence in Fluids: Stochastic and Numerical Modeling*, Kluwer, Dordrecht (1990).

Lozano, I., I. van Cruyningen, P. Danehy, and R. K. Hanson, "Planar Laser Induced Scalar Measurements in a Turbulent Jet," *Applications of Laser Techniques to Fluid Mechanics*, Vol. 19, R. J. Adrian, D. F. G. Durao, and F. Durst, eds., Springer-Verlag, Berlin (1986).

Paul, E. L., J. Mahadevan, J. Foster, and M. Kennedy Midler, "The Effect of Mixing on Scale-Up of a Parallel Reaction System," *Chem. Eng. Sci.*, **47**, 2837 (1992).

Rosenweig, R. F., "Idealized Theory for Turbulent Mixing in Vessels," *AIChE J.*, **10**, 91 (1964).

Schoenmakers, J. H. A., *Turbulent Feed Stream Mixing in Agitated Vessels*, PhD Thesis, Eindhoven Univ. of Technology, Eindhoven, The Netherlands (1998).

Schoenmakers, J. H. A., J. G. Wijers, and D. Thoenes, "Determination of Feed Stream Mixing Rates in Agitated Vessels," *Proc. Eur. Mix. Conf. (Paris): Récent Progrès en Génie des Procédés*, ed. Lavoisier Tec & Doc, **11**, 185 (1997).

Spalding, D. B., "Concentration Fluctuations in a Round Turbulent Free Jet," *Chem. Eng. Sci.*, **26**, 95 (1971).

Tennekes, H., and J. L. Lumley, *A First Course in Turbulence*, MIT Press, Cambridge, MA (1972).

Manuscript received May 1, 2001, and revision received Jan. 15, 2002.